



Lawrence Berkeley Laboratory

UNIVERSITY OF CALIFORNIA

Submitted to Physical Review C

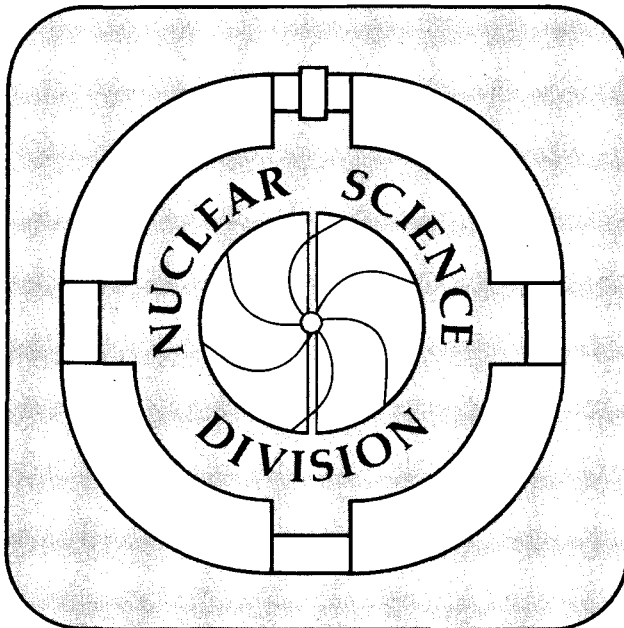
Systematic Analysis of Average Angular Momenta and Cross Sections in Subbarrier Fusion

D.E. DiGregorio and R.G. Stokstad

July 1990

For Reference

Not to be taken from this room



DISCLAIMER

This document was prepared as an account of work sponsored by the United States Government. While this document is believed to contain correct information, neither the United States Government nor any agency thereof, nor the Regents of the University of California, nor any of their employees, makes any warranty, express or implied, or assumes any legal responsibility for the accuracy, completeness, or usefulness of any information, apparatus, product, or process disclosed, or represents that its use would not infringe privately owned rights. Reference herein to any specific commercial product, process, or service by its trade name, trademark, manufacturer, or otherwise, does not necessarily constitute or imply its endorsement, recommendation, or favoring by the United States Government or any agency thereof, or the Regents of the University of California. The views and opinions of authors expressed herein do not necessarily state or reflect those of the United States Government or any agency thereof or the Regents of the University of California.

LBL-29297

**Systematic Analysis of Average Angular Momenta
and Cross Sections in Subbarrier Fusion**

D.E. DiGregorio and R.G. Stokstad

**Nuclear Science Division
Lawrence Berkeley Laboratory
University of California
Berkeley, CA 94720**

**This work was supported by the Director, Office of Energy Research,
Office of High Energy and Nuclear Physics, Nuclear Physics Division of
the U.S. Department of Energy under Contract No. DE-AC03-76SF00098.**

Systematic Analysis of Average Angular Momenta and Cross Sections in Subbarrier Fusion

D.E. DiGregorio[†] and R.G. Stokstad

Nuclear Science Division, Lawrence Berkeley Laboratory
1 Cyclotron Road, Berkeley, CA 94720

Abstract

Average angular momenta deduced from isomer ratio, gamma-multiplicity, and fission fragment angular anisotropy measurements, and the associated cross sections for fourteen systems are analyzed with a barrier penetration model that includes the coupling of inelastic channels. Good agreement was found between the theory and the data obtained from isomer ratio and from gamma-ray multiplicity measurements with the exception of the more symmetric systems. In these cases the discrepancies with theory show correlations in cross section and angular momentum suggesting that a valid model can be found. The measurements of angular momentum using the fission fragment anisotropy technique, however, do not appear reconcilable with the energy dependence of the cross sections. This systematic overview suggests that the origin of this discrepancy lies with the deduction of angular momentum from the measured anisotropy in inclusive fission fragment angular distributions.

PACS numbers: 25.70.Jj

I. INTRODUCTION

The measured cross sections for the fusion of heavy ions at energies near and below the Coulomb barrier can be orders of magnitude larger than the predictions of the one-dimensional barrier penetration model.¹⁻³ Theoretical studies of these enhancements have revealed the important role played by the nuclear structure of the colliding nuclei. Additional and complementary information has been obtained by measuring the moments of the angular momentum distributions leading to fusion deduced with three different techniques: gamma-multiplicity,⁴⁻¹⁰ fission fragment angular distributions¹¹⁻¹⁵ and very recently by measurements of isomer ratios.^{16,17} With the latter method it was possible to observe the predicted energy-independent lower limit for the average angular momentum, $\langle \ell \rangle$,¹⁶ and its expected variation with entrance channel.¹⁷ Measurements of the cross sections, $\sigma_{fus}(E)$, and the deduction of $\langle \ell \rangle$ by the isomer method are of interest because they provide an independent experimental approach to the problem that the theoretical values of $\langle \ell \rangle$ disagree with those deduced from fission fragment anisotropies and, sometimes, from gamma-ray multiplicities. This discrepancy has been an important and perhaps the central problem in studies of subbarrier fusion for several years.^{12,13,18-20} Theoretical models (e.g., Refs. 19-21) must account for both the measured subbarrier $\sigma_{fus}(E)$ and the $\langle \ell \rangle$. This double requirement places a strong constraint on a model because, within a given model, the angular momentum distribution, σ_ℓ , and the energy dependence of the cross section are intimately related.

We have investigated, following Ref. 22, all the presently available data on the first and second moments of the spin distributions leading to fusion and compared them to the *same* theoretical model. In addition, we analyze the corresponding experimental cross sections, since the starting point in an analysis of a fusion reaction should be the understanding of the excitation functions. A simplified coupled-channel code, CCFUS, has been used to perform all calculations.²³ This model has been used extensively in describing (mostly successfully) a large number of fusion excitation functions.³ We present an analysis of fourteen different systems: ${}^3\text{He} + {}^{136}\text{Ba}$ (Ref. 17), ${}^3\text{He} + {}^{137}\text{Ba}$ (Ref. 17), ${}^4\text{He} + {}^{136}\text{Ba}$ (Ref. 17), ${}^{12}\text{C} + {}^{128}\text{Te}$ (Refs. 16,17), ${}^{16}\text{O} + {}^{144}\text{Nd}$ (Refs. 6,10), ${}^{16}\text{O} + {}^{154}\text{Sm}$ (Refs. 4,5,22), ${}^{28}\text{Si} + {}^{154}\text{Sm}$ (Ref. 24), ${}^{64}\text{Ni} + {}^{96}\text{Zr}$ (Ref. 6), ${}^{80}\text{Se} + {}^{80}\text{Se}$ (Refs. 6,7), ${}^{64}\text{Ni} + {}^{100}\text{Mo}$ (Ref. 9), ${}^{16}\text{O} + {}^{208}\text{Pb}$ (Refs. 11,13,14), ${}^{12}\text{C} + {}^{236}\text{U}$ (Refs. 12,13), ${}^{16}\text{O} + {}^{232}\text{Th}$ (Refs. 12,13), and ${}^{19}\text{F} + {}^{232}\text{Th}$ (Ref. 15). For all these systems, the fusion cross sections and the first or second moments of their σ_ℓ distributions have been measured at different bombarding energies by one of the three experimental techniques mentioned above. For a few systems: ${}^{12}\text{C} + {}^{128}\text{Te}$ (Ref. 25), ${}^{16}\text{O} + {}^{144}\text{Nd}$ (Ref. 26), ${}^{16}\text{O} + {}^{154}\text{Sm}$ (Ref. 27), and ${}^{28}\text{Si} + {}^{154}\text{Sm}$ (Ref. 28), fusion excitation functions have been measured in independent experiments.

II. DEDUCTION OF THE MOMENTS OF THE SPIN DISTRIBUTION

The deduction of the moments of the spin distribution of the compound nucleus from the *measured quantities* is different for each experimental technique employed: isomer ratio measurements, gamma-ray multiplicity, and fission fragment angular distributions.

II. a. Isomer ratio

In the isomer ratio technique, the relationship between the spin distribution in the compound nucleus and the measured relative population of the ground and isomeric states in the evaporation residue is established through statistical model calculations.^{16,17,29} Starting with the experimental value of the isomer ratio, we deduce the average angular momentum of a smooth cutoff distribution for σ_ℓ represented by a Fermi function with fixed $\Delta\ell$ and variable ℓ_0 .¹⁷ The statistical calculations were performed with the use of the Monte Carlo code PACE,³⁰ which treats the effects of successive evaporation of neutrons leading to the evaporation residue, and the subsequent gamma-ray emission leading to the isomer or ground state. The code allows one to incorporate explicitly the low-lying levels of the residual nucleus and, thereby, to treat the last steps of the gamma-ray deexcitation realistically.

II. b. Gamma-ray multiplicity

Average gamma-ray multiplicities were obtained in early experiments,⁴⁻⁶ while the advent of detector arrays⁷⁻¹⁰ has made it possible to measure full multiplicity distributions. In either case, the measured multiplicities have to be converted to angular momenta to determine either the full σ_ℓ distribution or the $\langle \ell \rangle$. The conversions from the number of gamma-rays detected (coincidence fold) to multiplicity and then to angular momentum depend on instrumental effects such as the response function of the detector system and on a knowledge of the decay of a compound nucleus, respectively. Therefore, one needs to know the average angular momentum removed per photon, the average angular momentum carried off by the evaporated particles and the statistical gamma-rays, and the corrections for the internal conversion of the gamma-rays.^{8,9} Some of these quantities have been estimated using statistical model calculations.⁹

II. c. Fission fragment anisotropy

The second moment of the compound nuclear spin distribution can be obtained from the measured fission fragment angular distributions. In the standard transition-state theory³¹ the anisotropy of the fission fragment angular distribution is related approximately to the second moment of the spin distribution (mean-square spin) by the following expression,

$$\frac{W(180^\circ)}{W(90^\circ)} \simeq 1 + \frac{\langle \ell^2 \rangle}{4K_0^2}$$

where K_0 is the width of the distribution of the spin-projection along the symmetry axis and is determined by the nuclear temperature and the effective moment of inertia at the saddle point, $K_0^2 = J_{eff}T/\hbar^2$. By measuring the fission fragment anisotropies, the ratio $\langle \ell^2 \rangle / K_0^2$ can be determined, and thus one has to assume a value for K_0^2 to deduce $\langle \ell^2 \rangle$, or vice versa. At this point there are two approaches to follow in the interpretation of the anomalously large measured anisotropies. Vandenbosch et al.^{12,13,18} have deduced the value of K_0^2 from the above-barrier ${}^4\text{He} + {}^{244}\text{Cm}$ anisotropy³² in order to obtain $\langle \ell^2 \rangle$

for the reactions $^{12}\text{C} + ^{236}\text{U}$ and $^{16}\text{O} + ^{232}\text{Th}$ leading to the same compound nucleus, ^{248}Cf . Dasso et al.^{19,20}, however, argue that the energy dependence of the fusion cross section determines the content of σ_ℓ , and thus a model which describes $\sigma_{fus}(E)$ has to give reasonable values of $\langle \ell^2 \rangle$. Consequently, the large measured anisotropies should be taken as evidence for a small value of K_0^2 .

III. MODEL CALCULATIONS

The calculations of the fusion cross sections and angular momentum distributions are based on the matrix diagonalization method of Ref. 23 which solves the multi-dimensional barrier penetration problem and includes finite range effects. Its accuracy has been tested against exact coupled-channel numerical calculations.²³ The code can treat coupling to collective degrees of freedom (surface vibrations) of the target and/or projectile nuclei and to transfer channels. A new version of the program (CCDEF) has been implemented recently to treat static deformations in nuclei such as ^{154}Sm , ^{232}Th , and ^{236}U .³³ Coupling to transfer channels has not been included in any of the calculations presented in this work. The nuclear potential used in the code has a Wood-Saxon shape with parameters as given by Ref. 34. This potential together with the Coulomb potential determines the height and the curvature of the parabolic barrier.

The analysis of the systems $^{19}\text{F} + ^{232}\text{Th}$ (Ref. 15), $^{64}\text{Ni} + ^{100}\text{Mo}$ (Ref. 9), $^{12}\text{C} + ^{128}\text{Te}$ (Refs. 16,17), $^3\text{He} + ^{136,137}\text{Ba}$ (Ref. 17), and $^4\text{He} + ^{136}\text{Ba}$ (Ref. 17) with the CCFUS program is described in previous publications. For all other systems considered here the procedure was to: 1) determine the barrier parameters (V_b , R_b and $\hbar\omega$) for each system by adjusting the depth of the nuclear potential to fit the measured total fusion cross sections at energies above the Coulomb barrier; 2) include known values of electromagnetic transition probabilities for the lowest excited states of the target and/or projectile nuclei for each system.³⁵⁻³⁷

IV. COMPARISON BETWEEN EXPERIMENT AND THEORY

Figure 1 displays the ratio of the experimental fusion cross section, σ_{exp} , to the theoretical value, σ_{theo} , (upper frame) and the ratio of the experimental value, $\langle \ell \rangle_{exp}$, to the theoretical value, $\langle \ell \rangle_{theo}$, (lower frame) as a function of the ratio of the bombarding energy to the Coulomb barrier, for the isomer ratio measurements. Note that the cross sections and the average angular momenta for $^{12}\text{C} + ^{128}\text{Te}$, $^3\text{He} + ^{136}\text{Ba}$, $^3\text{He} + ^{137}\text{Ba}$, and $^4\text{He} + ^{136}\text{Ba}$ are fairly consistent with the theoretical expectations at bombarding energies above and well below the barrier.

In Fig. 2 we make a similar comparison for the gamma-ray multiplicity measurements. For the systems $^{28}\text{Si} + ^{154}\text{Sm}$, $^{16}\text{O} + ^{154}\text{Sm}$, and $^{16}\text{O} + ^{144}\text{Nd}$, both the σ_{exp} and the $\langle \ell \rangle_{exp}$ are well described by the CCFUS calculations. On the other hand, when the theory underestimates the cross section for $^{64}\text{Ni} + ^{100}\text{Mo}$ it also underestimates the average angular momentum. More precisely, it is the slope of the cross sections (the logarithmic derivative) that the theory overestimates. This corresponds to an underestimate of the

angular momentum, which is also observed. If the barrier can be approximated by a parabolic shape, then the mean square angular momentum and the energy dependence of the cross section are related by,²⁰

$$\langle \ell^2 \rangle = \frac{2\mu R_b^2}{\hbar^2} \epsilon, \quad \epsilon^{-1} = \frac{d}{dE} [\ln(E\sigma_{fus}(E))], \quad E \ll V_b.$$

Thus, the deviations of theory with experiment are in the *same direction* for both cross section and average angular momentum. Indeed, Halbert et al.⁹ have obtained a better fit to the cross sections and the angular momentum by increasing the strength of the coupling for all the inelastic channels by a factor of 1.5. Note that there is also a discrepancy between experiment and theory in the $\langle \ell \rangle$ values for $^{80}\text{Se} + ^{80}\text{Se}$ at energies below the barrier. Although the corresponding cross sections do not show a clear deviation, it is necessary to point out that only relative cross sections were reported in Ref. 7, and therefore, in the present analysis they have been arbitrarily normalized to the theory at bombarding energies above the barrier. In any case, it is apparent from this comparison that theory fails to satisfactorily describe the angular momentum and the cross sections at energies below the barrier for the more symmetric systems. Recently, Fröbrich et al.³⁸ have reported a consistent description of the measured $\sigma_{fus}(E)$ and $\langle \ell \rangle$ for $^{64}\text{Ni} + ^{100}\text{Mo}$ using a transport model for solving Langevin equations based on a surface friction model.

The comparison between theory and experiment for the case of fission fragment angular distributions is shown in Fig. 3. In this case we have plotted the ratio of the root-mean-square values, $\langle \ell^2 \rangle^{1/2}$, rather than the mean values. As noted by Vandenbosch,²² the ratios (experiment to theory) for the mean angular momentum and the ratios for the root-mean-square angular momentum are not very different for plausible σ_ℓ distributions. For $^{12}\text{C} + ^{236}\text{U}$ and $^{16}\text{O} + ^{232}\text{Th}$ the experimental values of $\langle \ell^2 \rangle$ are those given in Refs. 12 and 13, and were derived using empirical values of K_0^2 from the measured anisotropy of $^4\text{He} + ^{244}\text{Cm}$ (Ref. 32). For $^{16}\text{O} + ^{208}\text{Pb}$ (Refs. 11,13,14), and $^{19}\text{F} + ^{232}\text{Th}$ (Ref. 15), the values of $\langle \ell^2 \rangle$ were determined by deducing K_0^2 from the prediction of J_0/J_{eff} given by the diffuse surface liquid drop model of Sierk.³⁹ Figure 3 shows that the experimental cross sections are well reproduced by the CCFUS calculations, but that the theoretical root-mean-square values deviate significantly at energies around and below the barrier for all the systems. Given that the model reproduces the slope of the cross sections, it is hard to see how it can be so inconsistent with the average angular momentum. Similar conclusions were reached by Fröbrich et al..³⁸

On the other hand, if we follow the arguments of Refs. 19 and 20, we can take the values of $\langle \ell^2 \rangle$ given by the theory (since calculations with CCFUS reproduce the excitation function) and deduce values of K_0^2 from the measured anisotropies for $^{12}\text{C} + ^{236}\text{U}$, $^{16}\text{O} + ^{232}\text{Th}$, $^{16}\text{O} + ^{208}\text{Pb}$ and, as was done in Ref. 15, for $^{19}\text{F} + ^{232}\text{Th}$. Figure 4 shows the values of K_0 deduced in this approach for these four systems. We find that the values of K_0 are a factor of 2-3 smaller than those determined by using the values of J_0/J_{eff} of a rotating liquid drop given by Sierk's model.³⁹

The present analysis thus indicates that our overall theoretical understanding of the measured cross sections and fission fragment angular distributions is incomplete. Either one or more of the main elements - the calculations of fusion in the entrance channel, the assumption of the formation of an equilibrated compound nucleus, the assumptions in the standard transition-state model for fission, or the calculations of K_0^2 from the rotating liquid drop model - is not adequate.

Concerning the entrance channel, the prediction of the fusion cross sections for relatively light projectiles such as ^4He , ^{12}C , and ^{16}O is generally satisfactory for all three experimental methods. The assumption of compound nucleus formation followed by equilibrium fission would seem to be reasonable for the relatively asymmetric entrance channels, low angular momenta and excitation energies, and small values of $Z_1 Z_2$ encountered here. However, nonequilibrium or dynamic contributions to fission have been observed for much heavier systems such as $^{40}\text{Ar} + ^{197}\text{Au}$ (Ref. 40), and ^{40}Ar , ^{50}Ti , and $^{56}\text{Fe} + ^{208}\text{Pb}$ (Ref. 41,42). These reactions also show much larger anisotropies than expected on the basis of the transition-state model and, for mass-asymmetric fission decays, exhibit angular distributions that are asymmetric about 90° in the rest system. While it would seem unlikely that these quasi-fission mechanisms would persist for projectiles as light as ^{16}O , similar radiochemical measurements for reactions with lighter projectiles would be needed to rule out completely any nonequilibrium processes.

The use of empirical values of K_0 , deduced from the decay of the same compound nucleus populated in a light ion reaction at energies above the barrier^{12,13,32} (where one believes one knows the average angular momentum from the measured cross section), avoids the problem of calculating a value of K_0^2 from a model. Since such empirical values of K_0^2 tend to be smaller than the theoretical values, this reduces the discrepancy somewhat. Recent experimental studies^{43,44} show that corrections for the contributions from sequential fission (i.e., fission following transfer) to the fission fragment anisotropies reduce the discrepancies between experiment and theory, but they do not eliminate them.

Thus, we are left with a situation in which straight-forward entrance channel models for fusion (of ^4He , ^{12}C , and ^{16}O) are able to account for the cross sections and the average angular momenta with one exception - when the average angular momenta are deduced from fission fragment anisotropies. Barring unsuspected nonequilibrium contributions to fission, this suggests that the problem is in the deduction of angular momenta from measured fission anisotropies. The discrepancy is consistent with the fissioning system having a more elongated shape at the point where the distribution of K_0 becomes *fixed*. Indeed, the question of when and how the distribution of angular momenta projected along the symmetry axis is determined and fixed as the fissioning nucleus proceeds from saddle to scission has received extensive discussion.^{11,45-48}

V. CONCLUSIONS

In summary, we have analyzed all the existing data on the first or second moments of the spin distributions leading to fusion along with the corresponding experimental cross sections and compared them to the same model. All these calculations were performed with the coupled channel code, CCFUS.²³ A fairly good agreement was found between the theory and the data obtained from isomer ratio measurements and gamma-ray multiplicity for all the systems with the exception of the more symmetric ones, $^{64}\text{Ni} + ^{100}\text{Mo}$ and, less clearly, $^{80}\text{Se} + ^{80}\text{Se}$. In those cases when the theory overestimates the slope of the cross section it also underestimates the angular momentum. And finally, although the theoretical fusion-fission cross sections show very good agreement with experiment, there is a discrepancy with the average angular momenta. The present systematic overview suggests that the origin of the discrepancy may lie in the deduction of the angular momentum from the measured inclusive fission fragment angular distributions.

VI. ACKNOWLEDGMENTS

This work was supported by the Director, Office of Energy Research, Office of High Energy and Nuclear Physics, Nuclear Physics Division, of U.S. Department of Energy under Contract No. DE-AC03-76SF00098.

References

† Permanent address: Departamento de Física-TANDAR, Comisión Nacional de Energía Atómica, 1429 Buenos Aires, Argentina and CONICET.

1. M. Beckerman, *Phys. Rep.* **B129**, 145 (1985).
2. S.G. Steadman and M.J. Rhodes-Brown, *Ann. Rev. Nucl. Part. Sci.* **36**, 649 (1986).
3. C. Signorini et al., ed., *Proceedings of Symposium on Heavy Ion Interactions around the Coulomb Barrier*, Legnaro, Italy, June 1988, *Lecture Notes in Physics* Vol. 317, (Springer-Verlag, 1988).
4. R. Vandenbosch, B.B. Back, S. Gil, A. Lazzarini, and A. Ray, *Phys. Rev.* **C28**, 1161 (1983).
5. S. Gil, R. Vandenbosch, A.J. Lazzarini, D.-K. Lock and A. Ray, *Phys. Rev.* **C31**, 1752 (1985).
6. B. Haas, G. Duchêne, F.A. Beck, T. Byrski, C. Gehringer, J.C. Merdinger, A. Nourredine, V. Rauch, J.P. Vivien, J. Barrette, S. Tobbeche, E. Bozek, J. Styczen, J. Keinomen, J. Dudek, and W. Nazarewicz, *Phys. Rev. Lett.* **54**, 398 (1985).
7. P.J. Nolan, D.J.G. Love, A. Kirwan, D.J. Unwin, A.H. Nelson, P.J. Twin, J.D. Garret, *Phys. Rev. Lett.* **54**, 2211 (1985).
8. R.D. Fischer, A. Ruckelshausen, G. Koch, W. Kuhn, V. Metag, R. Muhlhans, R. Novotny, H. Stroher, H. Groger, D. Habs, H.W. Heyng, R. Repnow, D. Schwalm, W. Reisdorf and R.S. Simon, *Phys. Lett* **B171**, 33 (1986).
9. M.L. Halbert, J.R. Beene, D.C. Hensley, K. Honkanen, T.M. Semkow, V. Abenante, D.G. Sarantities, and Z. Li, *Phys. Rev.* **C40**, 2558 (1989).
10. G. Duchêne, P. Romain, S.K. Basu, F.A. Beck, Ph. Benet, E. Bozek, D.E. Di Gregorio, D. Disdier, J. Fernández Niello, B. Haas, B. Lott, V. Rauch, F. Scheibling, J.P. Vivien and K. Zuber, to be published.
11. B.B. Back, R.R. Betts, J.E. Gindler, B. D. Wilkins, S. Saini, M.B. Tsang, C.K. Gelbke, W.G. Lynch, M.A. McMahan, and P.A. Baisen, *Phys. Rev.* **C32**, 195 (1985).
12. R. Vandenbosch, T. Murakami, C.-C. Sahm, D.D. Leach, A. Ray and M.J. Murphy, *Phys. Rev. Lett.* **56**, 1234 (1986).
13. T. Murakami, C.-C. Sahm, R. Vandenbosch, D.D. Leach, A. Ray and M.J. Murphy, *Phys. Rev.* **C34**, 1353 (1986).
14. E. Vulgaris, L. Grodzins, S.G. Steadman, and R. Ledoux, *Phys. Rev.* **C33**, 2017 (1986).
15. H. Zhang, J. Xu, Z. Liu, J. Lu, K. Xu, and M. Ruan, *Phys. Lett.* **B218**, 133 (1989).

16. R.G. Stokstad, D.E. DiGregorio, K.T. Lesko, B.A. Harmon, E.B. Norman, J. Pouliot, and Y.D. Chan, *Phys. Rev. Lett.* **62**, 399 (1989).
17. D.E. DiGregorio, K.T. Lesko, B.A. Harmon, E.B. Norman, J. Pouliot, B. Sur, Y.D. Chan, and R.G. Stokstad, submitted to *Phys. Rev. C*.
18. R. Vandenbosch, T. Murakami, C.-C. Sahn, D.D. Leach, A. Ray and M.J. Murphy, *Phys. Rev. Lett.* **57**, 1499 (1986).
19. C.H. Dasso, H. Esbensen, and S. Landowne, *Phys. Rev. Lett.* **57**, 1498 (1986).
20. H. Esbensen and S. Landowne, *Nucl. Phys.* **A467**, 136 (1987).
21. C.H. Dasso and S. Landowne, *Phys. Rev.* **C32**, 1094 (1985).
22. R. Vandenbosch, Proceedings of Symposium on Heavy Ion Interactions around the Coulomb Barrier, Legnaro, Italy, June 1988, edited by C. Signorini et al., *Lecture Notes in Physics* Vol. 317, 157 (Springer-Verlag, 1988).
23. C.H. Dasso and S. Landowne, *Phys. Lett.* **B183**, 141 (1987); *Comp. Phys. Comm.* **46**, 187 (1987).
24. A.W. Charlop, A. Garcia, S. Gil, S. Kailas, S.J. Luke, D. Prindle, and R. Vandenbosch, to be published.
25. D.E. DiGregorio et al., to be published.
26. M. diTada et al., to be published.
27. R.G. Stokstad, Y. Eisen, S. Kaplanis, D. Pelte, U. Smilansky and I. Tserruya, *Phys. Rev. Lett.* **41**, 465 (1978); *Phys. Rev.* **C21**, 2427 (1980).
28. S. Gil et al., Proceedings on the XII Workshop on Nuclear Physics, Iguazú Falls, Argentina, 1989, World Scientific Publishing Co, Singapore 1990, p. 44.
29. R.G. Stokstad, "The Use of Statistical Models in Heavy-Ion Reaction Studies" in *Treatise on Heavy-Ion Science*, Vol. 3, edited by D.M. Bromley, Plenum (1985).
30. A. Gavron, *Phys. Rev.* **C21**, 230 (1980).
31. R. Vandenbosch and J.R. Huizenga, *Nuclear Fission*, (Academic, New York, 1973).
32. R. F. Reising, G.L. Bate, and J.R. Huizenga, *Phys. Rev.* **141**, 1161 (1966).
33. J.O. Fernández Niello, C.H. Dasso and S. Landowne, *Comp. Phys. Comm.* **54**, 409 (1989).
34. P.R. Christensen and A. Winther, *Phys. Lett.* **B65**, 19 (1976).
35. P.M. Endt, *Atomic Data and Nucl. Data Tables* **23**, 3 and 547 (1979).
36. S. Raman, C.H. Malarkey, W.T. Milner, C.W. Nestor, Jr., and P.H. Stelson, *Atomic Data and Nucl. Data Tables*, **36**, 1 (1987).
37. R.M. Spear, *Atomic Data and Nucl. Data Tables* **42**, 55 (1989).

38. P. Fröbrich and J. Richert, Phys. Lett. **B237**, 328 (1990).
39. A. Sierk, Phys. Rev. **C33**, 2039 (1986).
40. H. Schulte, B. Jäckel, R.A. Esterlund, M. Knaack, W. Westmeier, A. Rox, and P. Patzelt, Phys. Lett. **B232**, 37 (1989).
41. K. Lützenkirchen, J.V. Kratz, G. Wirth, W. Brüche, L. Dörr, K. Sümmerer, R. Lucas, J. Poitou, C. Grégoire, and S. Bjornholm, Z. Phys. **A320**, 529 (1985); Nucl. Phys. **A452**, 351 (1986).
42. H. Keller, K. Lützenkirchen, J.V. Kratz, G. Wirth, W. Brüche, and K. Sümmerer, Z. Phys. **A326**, 313 (1987).
43. J.P. Lestone, J.R. Lehigh, J.O. Newton, and J.X. Wei, Preprint, Australian National University, Canberra (1989).
44. B.B. Back, R.R. Betts, P. Fernández, B.G. Glagola, T. Happ, D. Henderson, H. Ikezoe, and Ph. Benet, Preprint, "Sixth Winter Workshop on Nuclear Dynamics", Jackson Hole, Wyoming, February 17-24, 1990.
45. P.D. Bond, Phys. Rev. Lett., **52**, 414 (1984).
46. B.B. Back, Phys. Rev. **C31**, 2140 (1985).
47. H.H. Rossner, J.R. Huizenga, and W.U. Schröder, Phys. Rev. Lett., **53**, 38 (1984).
48. M. Prakash, V.S. Ramamurthy, S.S. Kapoor, and J.M. Alexander, Phys. Rev. Lett., **52**, 990 (1984).

Figure Captions

Fig. 1. Comparison of experimental and theoretical cross sections, and average angular momenta, as a function of bombarding energy relative to the Coulomb barrier for the results of isomer ratio measurements.

Fig. 2. Same as Fig.1 but for gamma-multiplicity measurements.

Fig. 3. Same as Fig.1 but for fission fragment anisotropy measurements.

Fig. 4. Values of K_0 deduced from the measured fission fragment anisotropies and $\langle \ell^2 \rangle$ calculated from CCFUS,²³ as a function of the ratio of bombarding energy to the Coulomb barrier. The solid lines represent the values of K_0 calculated with J_0/J_{eff} obtained from Sierk's model.³⁹

Isomer ratio

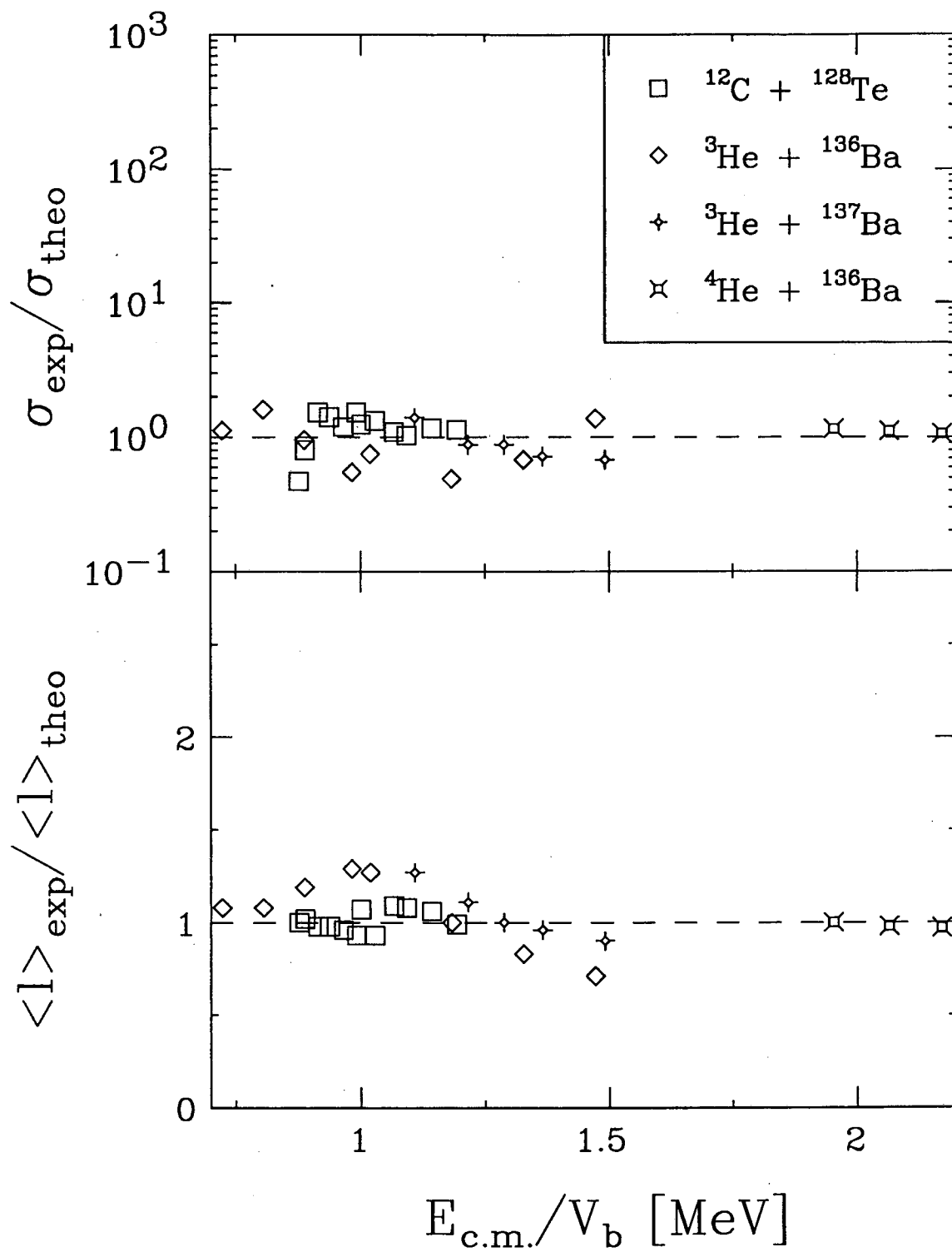


Figure 1

γ -Multiplicity

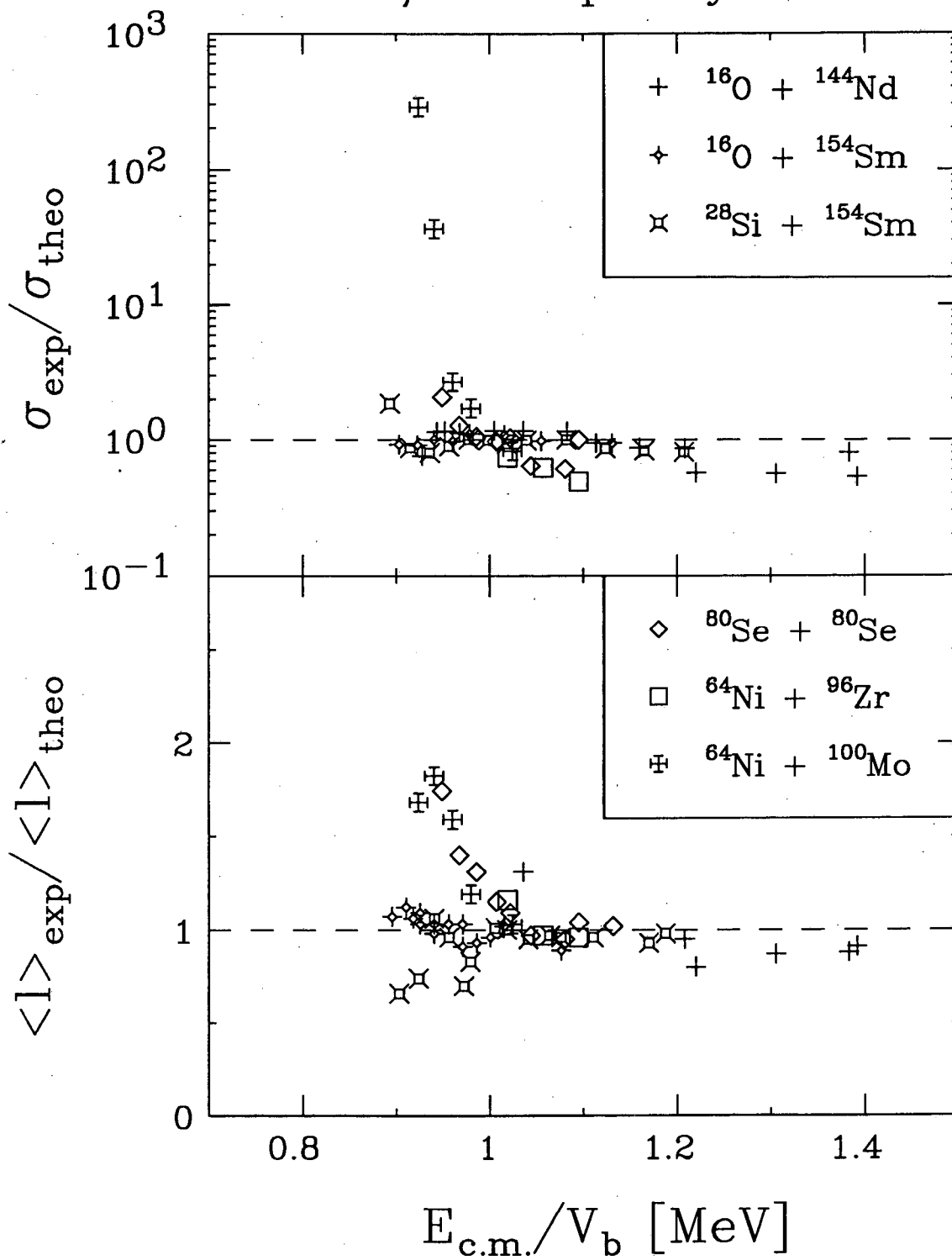


Figure 2

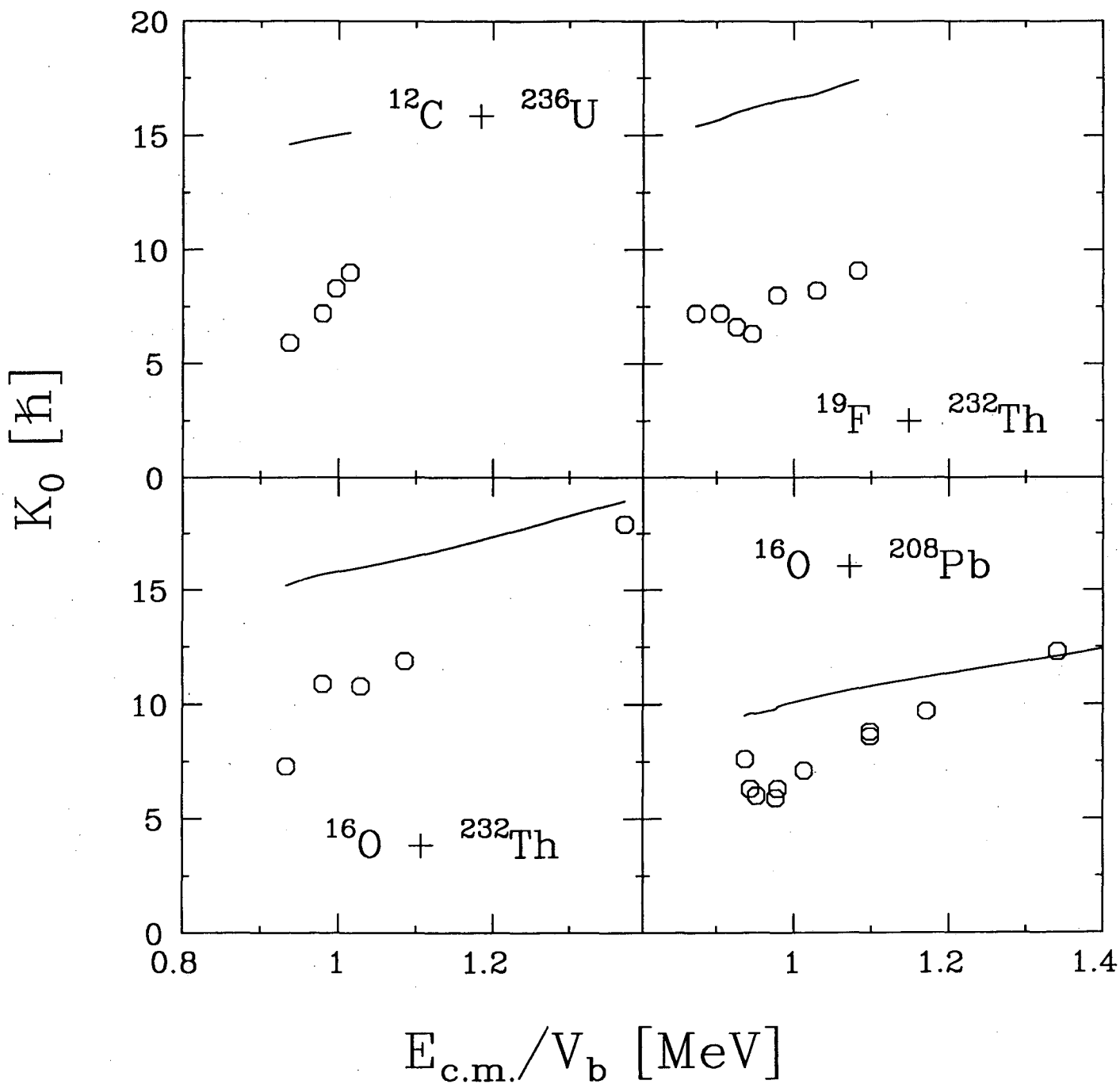


Figure 4

LAWRENCE BERKELEY LABORATORY
UNIVERSITY OF CALIFORNIA
INFORMATION RESOURCES DEPARTMENT
BERKELEY, CALIFORNIA 94720